Journal of Computational and Applied Mathematics 388 (2021) 113296

Contents lists available at ScienceDirect

Journal of Computational and Applied Mathematics

journal homepage: www.elsevier.com/locate/cam

Geometric Hermite interpolation by a family of spatial algebraic–trigonometric PH curves

Weidong Wu [a], Xunnian Yang [b,*]

[a] School of Mathematics and Statistics, Shandong University of Technology, Zibo 255049, China
[b] School of Mathematical Sciences, Zhejiang University, Hangzhou 310027, China

ARTICLE INFO

Article history:
Received 17 August 2019
Received in revised form 14 September 2020

Keywords:
Algebraic–trigonometric PH curves
Hermite interpolation
Arc length

ABSTRACT

This paper proposes to define a family of spatial algebraic–trigonometric Pythagorean Hodograph (ATPH) curves by integrals of scaled unit tangent vector fields which are originally defined as sphere curves. The obtained ATPH curves have only polynomial parametric speeds but the curves can be employed to represent several typical non-polynomial curves without rational form. A simple algorithm for geometric Hermite interpolation by the proposed spatial ATPH curves without or with arc length constraint has been given. Given two boundary points and two unit tangents at the points, possibly with a prescribed arc length, a unique interpolating ATPH curve can be obtained by solving a simple linear system.

1. Introduction

Among all parametric curves those with polynomial parametric speeds or polynomial arc lengths play particular roles in geometric modeling and CNC machining [1–3]. In the past few decades polynomial curves with Pythagorean Hodographs (shortly PH curves) and their applications in geometric modeling have been studied extensively [4–8]. More theories and algorithms about PH curves can be found in the book [9] or a recent survey paper [10].

Though non-uniform rational B-spline (NURBS) as well as B-spline, Bézier or rational Bézier curves are popular tools for geometric modeling, they have to represent typical curves like circles in rational form [11]. Transcendental curves such as cycloid, catenary, etc. even cannot be represented exactly by NURBS or other polynomial based curves. To represent circles and other transcendental curves simply and exactly, Pottmann [12,13] defined a class of helix splines over a mixed space of polynomials and trigonometric functions. Straight lines, circles and helices can be represented by helix splines with arc-length parametrization. Similarly, Zhang [14,15] introduced the C–B-splines in the space $\Omega = span\{1, t, \cos t, \sin t\}$, as the extensions of cubic uniform B-splines. Several types of non-polynomial curves for shape preserving design have been given in [16–19].

Similar to PH curves constructed in polynomial spaces, PH-like curves can also be constructed in non-polynomial spaces. Romani et al. [20] introduced the ATPH curves defined over a mixed algebraic–trigonometric space $\Omega = span\{\sin t, \cos t, \sin 2t, \cos 2t, 1, t\}$. ATPH curves have similar properties as conventional PH curves and can be used for C^1 Hermite interpolation. While polynomial PH curves have rational offsets and polynomial arc lengths, the arc-lengths of ATPH curves are trigonometric functions and their offsets are rational curves represented by mixed algebraic–trigonometric functions. ATPH curves can also be used for possible applications in CNC machining or other modeling

* Corresponding author.
E-mail address: yxn@zju.edu.cn (X. Yang).

https://doi.org/10.1016/j.cam.2020.113296
0377-0427/

purposes. Besides single curve segments, González et al. [21] employed the ATPH curves for the construction of a planar C^2 spline curve. By exploring algebraic conditions similar to polynomial space PH curves, ATPH space curves represented by algebraic and trigonometric polynomials have been proposed in [22].

Besides satisfying algebraic conditions, ATPH curves can also be constructed in a geometric way. Wu and Yang [23] introduced a family of intrinsically defined planar curves within space $\Omega = span\{1, \sin\theta, \cos\theta, \theta\sin\theta, \ldots, \theta^n\cos\theta\}$. The curves are locally convex and the offsets to the curves lie in the same space. When the curvature radius functions are polynomials in terms of the tangent angle, the Cartesian coordinates of the curves can be explicitly obtained by the integral of scaled tangent vector fields. If the prescribed unit tangent vector fields are represented by rational Bézier curves, convex PH curves or PH curves with single inflection points can be constructed by integrals of the scaled tangent vector fields [8].

In this paper we propose to construct spatial ATPH curves by integrals of hodographs which are originally given as scaled unit tangent vector fields in 3D space. These types of ATPH curves have only polynomial parametric speeds and polynomial arc lengths. Since the curves are defined in a mixed space of polynomials and trigonometric functions, several typical non-polynomial curves can be represented by the proposed model exactly. Based on their definition, geometric Hermite interpolation by the proposed spatial ATPH curves without or with arc length constraint can be implemented in two steps: unit tangent vector field construction and scaling function computation. For both of the two steps, only simple linear systems should be solved and unique interpolating curves can be obtained.

The remainder of the paper is organized as follows: In Section 2, we define a family of spatial integral curves with polynomial arc lengths. Section 3 introduces the technique of G^1 Hermite interpolation by the proposed curve model. Given G^1 Hermite data together with an arc-length, algorithm for construction of an interpolating PH curve with the prescribed arc-length will be presented in Section 4. Section 5 concludes the paper.

2. A family of spatial ATPH curves with non-rational unit tangents

In this section, we propose to define a family of spatial ATPH curves that have non-rational unit tangent vectors. Particularly, the unit tangent vectors are represented by spherical curves using spherical coordinates. When the magnitudes of hodographs of the curves are chosen simple elementary functions, explicit Cartesian coordinates of the curves are obtained.

Assume that a_0, a_1, b_0 and b_1 are real numbers and $a_1^2 + b_1^2 \neq 0$, a spherical curve is given by

$$\mathbf{T}(\xi) = \begin{pmatrix} \cos(a_1\xi + a_0)\cos(b_1\xi + b_0) \\ \cos(a_1\xi + a_0)\sin(b_1\xi + b_0) \\ \sin(a_1\xi + a_0) \end{pmatrix}, \quad \xi \in [0, 1]. \tag{2.1}$$

Based on the definition of $\mathbf{T}(\xi)$ we know that $\mathbf{T}(0) = (\cos a_0 \cos b_0, \cos a_0 \sin b_0, \sin a_0)^T$ and $\mathbf{T}(1) = (\cos(a_1 + a_0)\cos(b_1 + b_0), \cos(a_1 + a_0)\sin(b_1 + b_0), \sin(a_1 + a_0))^T$, where the upper letter "T" means the transpose of a vector or a matrix. When $\mathbf{T}(\xi)$ is obtained, a spatial curve that has prescribed unit tangent vector field $\mathbf{T}(\xi)$ is given by

$$\mathbf{r}(\xi) = \int_0^\xi \rho(t)\mathbf{T}(t)dt + \mathbf{r}_0, \quad \xi \in [0, 1], \tag{2.2}$$

where $\rho(t)$ can be chosen any integrable real function and $\mathbf{r}_0$ is an arbitrary point in $\mathbb{R}^3$. From the definition of $\mathbf{r}(\xi)$ we know that the curve $\mathbf{r}(\xi)$ is a planar curve if and only if the unit tangent vector field $\mathbf{T}(\xi)$ lies on a plane. Particularly, it can be easily verified that the unit tangent vector field given by Eq. (2.1) lies on a plane that passes through the origin when $a_1 = a_0 = 0$ or $b_1 = 0$. Techniques for constructing a ATPH curve from a planar tangent vector field can be found in [23].

Let $A_1 = a_1 + b_1$, $A_0 = a_0 + b_0$, $B_1 = a_1 - b_1$, $B_0 = a_0 - b_0$. The Cartesian coordinates of the curve $\mathbf{r}(\xi)$ are formulated as

$$\begin{aligned} \mathbf{r}(\xi) &= \begin{pmatrix} x(\xi) \\ y(\xi) \\ z(\xi) \end{pmatrix} \\ &= \begin{pmatrix} \int_0^\xi \rho(t)\cos(a_1t + a_0)\cos(b_1t + b_0)dt \\ \int_0^\xi \rho(t)\cos(a_1t + a_0)\sin(b_1t + b_0)dt \\ \int_0^\xi \rho(t)\sin(a_1t + a_0)dt \end{pmatrix} + \mathbf{r}_0 \\ &= \begin{pmatrix} \frac{1}{2}\int_0^\xi \rho(t)\cos(A_1t + A_0)dt + \frac{1}{2}\int_0^\xi \rho(t)\cos(B_1t + B_0)dt \\ \frac{1}{2}\int_0^\xi \rho(t)\sin(A_1t + A_0)dt - \frac{1}{2}\int_0^\xi \rho(t)\sin(B_1t + B_0)dt \\ \int_0^\xi \rho(t)\sin(a_1t + a_0)dt \end{pmatrix} + \mathbf{r}_0. \end{aligned} \tag{2.3}$$

Particularly, the coordinates of $\mathbf{r}(\xi)$ can be explicitly computed when $\rho(t)$ is chosen as any elementary function. Because $\|\mathbf{r}'(\xi)\| = |\rho(\xi)|$, the arc length of the spatial curve $\mathbf{r}(\xi)$ is obtained as $L(\xi) = \int_0^\xi |\rho(t)|dt$.

From Eq. (2.2), the unit normal $\mathbf{N}(\xi)$ and the binormal $\mathbf{B}(\xi)$ of the curve are derived as

$$\mathbf{N}(\xi) = \frac{\mathbf{T}'(\xi)}{\|\mathbf{T}'(\xi)\|},$$
$$\mathbf{B}(\xi) = \mathbf{T}(\xi) \times \mathbf{N}(\xi) = \frac{\mathbf{T}(\xi) \times \mathbf{T}'(\xi)}{\|\mathbf{T}(\xi) \times \mathbf{T}'(\xi)\|}.$$

The curvature and the torsion of the curve $\mathbf{r}(\xi)$ are obtained as follows:

$$k(\xi) = \frac{\|\mathbf{r}'(\xi) \times \mathbf{r}''(\xi)\|}{\|\mathbf{r}'(\xi)\|^3} = \frac{\|\mathbf{T}(\xi) \times \mathbf{T}'(\xi)\|}{|\rho(\xi)|}$$

and

$$\tau(\xi) = \frac{det(\mathbf{r}'(\xi), \mathbf{r}''(\xi), \mathbf{r}'''(\xi))}{\|\mathbf{r}'(\xi) \times \mathbf{r}''(\xi)\|^2} = \frac{det(\mathbf{T}(\xi), \mathbf{T}'(\xi), \mathbf{T}''(\xi))}{|\rho(\xi)|\|\mathbf{T}(\xi) \times \mathbf{T}'(\xi)\|^2}.$$

Based on the curvature and torsion formulae, the regularity of the curve $\mathbf{r}(\xi)$ can be checked by the sign of $\rho(t)$ directly.

Proposition 1. *If $\rho(t) \neq 0$, for $0 \leq t \leq 1$, then the spatial ATPH curve defined by Eq. (2.2) is non-singular.*

In this paper we choose $\rho(t)$ as quadratic or cubic polynomials such that the obtained ATPH curves have enough degrees of freedom to interpolate prescribed Hermite data or arc lengths. Firstly, the integral function $\rho(t)$ is chosen as a quadratic function

$$\rho(t) = \rho_{II}(t) = bt^2 + ct + d, \quad t \in [0, 1], \tag{2.4}$$

where b, c and d are real constants. Substituting Eq. (2.4) into Eq. (2.3), the coordinates of the curve can be computed as follows:

$$\mathbf{r}(\xi) = \begin{pmatrix} \frac{1}{2}(B_x(\xi)b + C_x(\xi)c + D_x(\xi)d) \\ \frac{1}{2}(B_y(\xi)b + C_y(\xi)c + D_y(\xi)d) \\ B_z(\xi)b + C_z(\xi)c + D_z(\xi)d \end{pmatrix} + \mathbf{r}_0, \tag{2.5}$$

where

$$\begin{aligned}
B_x(\xi) = {} & (\tfrac{1}{A_1}\xi^2 - \tfrac{2}{A_1^3})\sin(A_1\xi + A_0) + \tfrac{2}{A_1^2}\xi\cos(A_1\xi + A_0) + \tfrac{2}{A_1^3}\sin(A_0) \\
& + (\tfrac{1}{B_1}\xi^2 - \tfrac{2}{B_1^3})\sin(B_1\xi + B_0) + \tfrac{2}{B_1^2}\xi\cos(B_1\xi + B_0) + \tfrac{2}{B_1^3}\sin(B_0), \\
C_x(\xi) = {} & \tfrac{1}{A_1}\xi\sin(A_1\xi + A_0) + \tfrac{1}{A_1^2}\cos(A_1\xi + A_0) - \tfrac{1}{A_1^2}\cos(A_0) \\
& + \tfrac{1}{B_1}\xi\sin(B_1\xi + B_0) + \tfrac{1}{B_1^2}\cos(B_1\xi + B_0) - \tfrac{1}{B_1^2}\cos(B_0), \\
D_x(\xi) = {} & \tfrac{1}{A_1}\sin(A_1\xi + A_0) - \tfrac{1}{A_1}\sin(A_0) + \tfrac{1}{B_1}\sin(B_1\xi + B_0) - \tfrac{1}{B_1}\sin(B_0), \\
B_y(\xi) = {} & (-\tfrac{1}{A_1}\xi^2 + \tfrac{2}{A_1^3})\cos(A_1\xi + A_0) + \tfrac{2}{A_1^2}\xi\sin(A_1\xi + A_0) - \tfrac{2}{A_1^3}\cos(A_0) \\
& - [(-\tfrac{1}{B_1}\xi^2 + \tfrac{2}{B_1^3})\cos(B_1\xi + B_0) + \tfrac{2}{B_1^2}\xi\sin(B_1\xi + B_0) - \tfrac{2}{B_1^3}\cos(B_0)], \\
C_y(\xi) = {} & -\tfrac{1}{A_1}\xi\cos(A_1\xi + A_0) + \tfrac{1}{A_1^2}\sin(A_1\xi + A_0) - \tfrac{1}{A_1^2}\sin(A_0) \\
& - [-\tfrac{1}{B_1}\xi\cos(B_1\xi + B_0) + \tfrac{1}{B_1^2}\sin(B_1\xi + B_0) - \tfrac{1}{B_1^2}\sin(B_0)], \\
D_y(\xi) = {} & -\tfrac{1}{A_1}\cos(A_1\xi + A_0) + \tfrac{1}{A_1}\cos(A_0) - [-\tfrac{1}{B_1}\cos(B_1\xi + B_0) + \tfrac{1}{B_1}\cos(B_0)], \\
B_z(\xi) = {} & (-\tfrac{1}{a_1}\xi^2 + \tfrac{2}{a_1^3})\cos(a_1\xi + a_0) + \tfrac{2}{a_1^2}\xi\sin(a_1\xi + a_0) - \tfrac{2}{a_1^3}\cos(a_0), \\
C_z(\xi) = {} & -\tfrac{1}{a_1}\xi\cos(a_1\xi + a_0) + \tfrac{1}{a_1^2}\sin(a_1\xi + a_0) - \tfrac{1}{a_1^2}\sin(a_0), \\
D_z(\xi) = {} & -\tfrac{1}{a_1}\cos(a_1\xi + a_0) + \tfrac{1}{a_1}\cos(a_0).
\end{aligned}$$

Secondly, we choose $\rho(t)$ as a cubic function $\rho(t) = \rho_{III}(t) = at^3 + bt^2 + ct + d$. By a simple computation it yields

$$\mathbf{r}(\xi) = \begin{pmatrix} \frac{1}{2}(A_x(\xi)a + B_x(\xi)b + C_x(\xi)c + D_x(\xi)d) \\ \frac{1}{2}(A_y(\xi)a + B_y(\xi)b + C_y(\xi)c + D_y(\xi)d) \\ A_z(\xi)a + B_z(\xi)b + C_z(\xi)c + D_z(\xi)d \end{pmatrix} + \mathbf{r}_0, \tag{2.6}$$

where

$$\begin{aligned}
A_x(\xi) = \;& (\tfrac{1}{A_1}\xi^3 - \tfrac{6}{A_1^3}\xi)\sin(A_1\xi + A_0) + (\tfrac{3}{A_1^2}\xi^2 - \tfrac{6}{A_1^4})\cos(A_1\xi + A_0) + \tfrac{6}{A_1^4}\cos(A_0) \\
& + (\tfrac{1}{B_1}\xi^3 - \tfrac{6}{B_1^3}\xi)\sin(B_1\xi + B_0) + (\tfrac{3}{B_1^2}\xi^2 - \tfrac{6}{B_1^4})\cos(B_1\xi + B_0) + \tfrac{6}{B_1^4}\cos(B_0), \\
A_y(\xi) = \;& (-\tfrac{1}{A_1}\xi^3 + \tfrac{6}{A_1^3}\xi)\cos(A_1\xi + A_0) + (\tfrac{3}{A_1^2}\xi^2 - \tfrac{6}{A_1^4})\sin(A_1\xi + A_0) + \tfrac{6}{A_1^4}\sin(A_0) \\
& - [(-\tfrac{1}{B_1}\xi^3 + \tfrac{6}{B_1^3}\xi)\cos(B_1\xi + B_0) + (\tfrac{3}{B_1^2}\xi^2 - \tfrac{6}{B_1^4})\sin(B_1\xi + B_0) + \tfrac{6}{B_1^4}\sin(B_0)], \\
A_z(\xi) = \;& (-\tfrac{1}{a_1}\xi^3 + \tfrac{6}{a_1^3}\xi)\cos(a_1\xi + a_0) + (\tfrac{3}{a_1^2}\xi^2 - \tfrac{6}{a_1^4})\sin(a_1\xi + a_0) + \tfrac{6}{a_1^4}\sin(a_0),
\end{aligned}$$

and the remaining terms are as defined in Eq. (2.5).

In Eqs. (2.5) and (2.6), we assume that $a_1 \neq 0, A_1 \neq 0$ and $B_1 \neq 0$. When one of them is zero, it is simple to recompute the formulae of the integral curve.

We reformulate the quadratic function $\rho(t)$ as follows:

$$\begin{aligned}
\rho_{II}(t) &= bt^2 + ct + d \\
&= \rho_0 B_0^2(t) + \rho_1 B_1^2(t) + \rho_2 B_2^2(t), \;\; t \in [0, 1],
\end{aligned} \tag{2.7}$$

where $\rho_0 = d$, $\rho_1 = d + \frac{1}{2}c$, $\rho_2 = d + c + b$ and $B_i^2(t) = \frac{2!}{i!(2-i)!}t^i(1-t)^{2-i}$, $i = 0, 1, 2$, are the Bernstein basis functions.

Substituting Eq. (2.7) into Eq. (2.5), the coordinates of the curve can be computed as follows:

$$\mathbf{r}(\xi) = \begin{pmatrix} \frac{1}{2}\Big(B_x(\xi)\rho_2 + (-2B_x(\xi) + 2C_x(\xi))\rho_1 + (B_x(\xi) - 2C_x(\xi) + D_x(\xi))\rho_0\Big) \\ \frac{1}{2}\Big(B_y(\xi)\rho_2 + (-2B_y(\xi) + 2C_y(\xi))\rho_1 + (B_y(\xi) - 2C_y(\xi) + D_y(\xi))\rho_0\Big) \\ B_z(\xi)\rho_2 + (-2B_z(\xi) + 2C_z(\xi))\rho_1 + (B_z(\xi) - 2C_z(\xi) + D_z(\xi))\rho_0 \end{pmatrix} + \mathbf{r}_0, \tag{2.8}$$

Similarly, the cubic function $\rho_{III}(t)$, $t \in [0, 1]$, can be represented in Bernstein–Bézier form as follows:

$$\rho_{III}(t) = l_0 B_0^3(t) + l_1 B_1^3(t) + l_2 B_2^3(t) + l_3 B_3^3(t), \quad t \in [0, 1], \tag{2.9}$$

where

$$\begin{cases} l_0 = d, \\ l_1 = d + \frac{1}{3}c, \\ l_2 = d + \frac{2}{3}c + \frac{1}{3}b, \\ l_3 = d + c + b + a. \end{cases}$$

Substituting Eq. (2.9) into Eq. (2.6), the coordinates of the curve can be computed as follows:

$$\mathbf{r}(\xi) = \begin{pmatrix} \frac{1}{2}(G_{11}(\xi)l_3 + G_{12}(\xi)l_2 + G_{13}(\xi)l_1 + G_{14}(\xi)l_0) \\ \frac{1}{2}(G_{21}(\xi)l_3 + G_{22}(\xi)l_2 + G_{23}(\xi)l_1 + G_{24}(\xi)l_0) \\ G_{31}(\xi)l_3 + G_{32}(\xi)l_2 + G_{33}(\xi)l_1 + G_{34}(\xi)l_0 \end{pmatrix} + \mathbf{r}_0, \tag{2.10}$$

where

$$\begin{aligned}
G_{11}(\xi) &= A_x(\xi), \\
G_{12}(\xi) &= -3A_x(\xi) + 3B_x(\xi), \\
G_{13}(\xi) &= 3A_x(\xi) - 6B_x(\xi) + 3C_x(\xi), \\
G_{14}(\xi) &= -A_x(\xi) + 3B_x(\xi) - 3C_x(\xi) + D_x(\xi), \\
G_{21}(\xi) &= A_y(\xi), \\
G_{22}(\xi) &= -3A_y(\xi) + 3B_y(\xi), \\
G_{23}(\xi) &= 3A_y(\xi) - 6B_y(\xi) + 3C_y(\xi), \\
G_{24}(\xi) &= -A_y(\xi) + 3B_y(\xi) - 3C_y(\xi) + D_y(\xi), \\
G_{31}(\xi) &= A_z(\xi), \\
G_{32}(\xi) &= -3A_z(\xi) + 3B_z(\xi), \\
G_{33}(\xi) &= 3A_z(\xi) - 6B_z(\xi) + 3C_z(\xi), \\
G_{34}(\xi) &= -A_z(\xi) + 3B_z(\xi) - 3C_z(\xi) + D_z(\xi).
\end{aligned}$$

Fig. 1 illustrates a family of spatial integral curves which are defined by quadratic polynomial and trigonometric functions. Given a unit tangent vector field in advance, three ATPH curves are obtained by Eq. (2.5) when different polynomial functions $\rho(t)$ have been chosen for the integral. Particularly, the curves in red, green or blue colors are

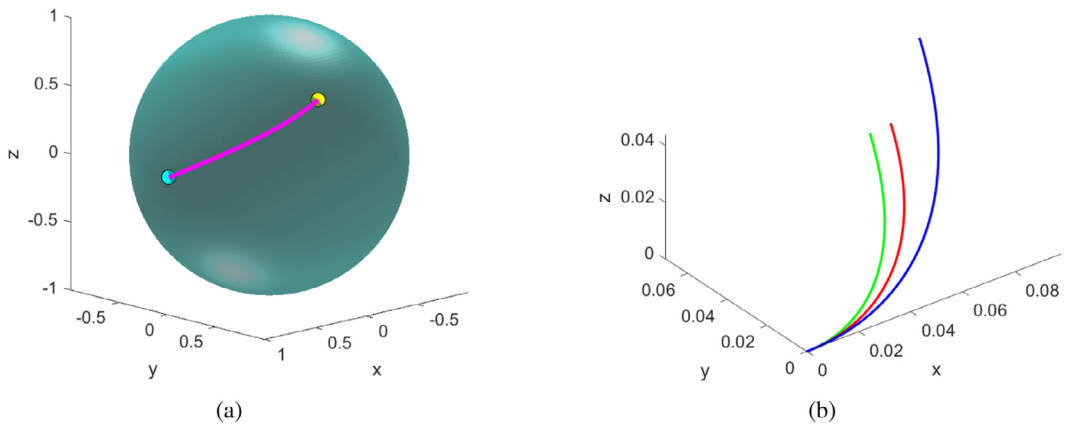

Fig. 1. (a) The unit tangent vector field constructed by Eq. (2.1) with $a_1 = 0.2\pi$, $a_0 = 0$, $b_1 = 0.4\pi$, $b_0 = 0$, $t \in [0, 1]$; (b) spatial ATPH curves computed by integrals of scaled tangent vector fields. (For interpretation of the references to color in this figure legend, the reader is referred to the web version of this article.)

obtained by choosing $\rho(t) = (0.002\pi^2)t^2 + (0.01\pi)t + 0.3$, $\rho(t) = (0.001\pi^2)t^2 + (0.06\pi)t + 0.2$ or $\rho(t) = (0.003\pi^2)t^2 + (0.02\pi)t + 0.4$, respectively, all with $\mathbf{r}_0 = 0$. This example shows that it is possible to interpolate an ATPH curve to G^1 Hermite data by first interpolating the boundary tangent vectors and then computing a scaling function for the integral.

3. G^1 Hermite Interpolation

In this section we present concrete algorithm steps for solving the G^1 Hermite interpolation problem using the spatial ATPH curves defined in Section 2. Suppose that $\{\mathbf{P}_1, \mathbf{T}_1; \mathbf{P}_2, \mathbf{T}_2\}$ are the given boundary points and the unit tangents at the points, we construct an interpolating spatial ATPH curve by choosing a quadratic polynomial $\rho_{II}(\xi)$ for the integral (2.2). The algorithm consists of two main steps. First, we compute a unit tangent vector field based on the two given boundary tangent vectors. After then, we compute the unknown parameters within $\rho_{II}(\xi)$ based on the end interpolation condition.

3.1. Compute the interpolating unit tangent vector field

As a first step of the proposed Hermite interpolation algorithm, we compute a spherical curve $\mathbf{T}(\xi)$ that interpolates given tangents $\mathbf{T}_1$ and $\mathbf{T}_2$ at the ends. Assume the Cartesian coordinates of the given tangent vectors are $\mathbf{T}_i = (t_{i1}, t_{i2}, t_{i3})$, $i = 1, 2$, we represent the vectors by spherical coordinates as $\mathbf{T}_i = (\cos\theta_i \cos\phi_i, \cos\theta_i \sin\phi_i, \sin\theta_i)$, $i = 1, 2$. Particularly, the angle θ_i is computed by $\theta_i = \arcsin(t_{i3})$ and the angle ϕ_i is given by

$$\phi_i = \begin{cases} \arctan(\frac{t_{i2}}{t_{i1}}), & \text{if} \quad t_{i1} > 0, \\ \arctan(\frac{t_{i2}}{t_{i1}}) + \pi, & \text{if} \quad t_{i1} < 0, \\ +\frac{\pi}{2}, & \text{if} \quad t_{i1} = 0, t_{i2} > 0, \\ -\frac{\pi}{2}, & \text{if} \quad t_{i1} = 0, t_{i2} < 0, \end{cases}$$

for $i = 1, 2$. If $t_{i1} = t_{i2} = 0$, the unit tangent vector $\mathbf{T}_i$ becomes $\mathbf{T}_i = (0, 0, 1)$ or $\mathbf{T}_i = (0, 0, -1)$. In this case, the angle ϕ_i can be chosen any real number.

Based on the assumption that a unit tangent vector curve $\mathbf{T}(\xi)$ interpolates given boundary tangents, i.e., $\mathbf{T}(0) = \mathbf{T}_1$ and $\mathbf{T}(1) = \mathbf{T}_2$, we have

$$\begin{cases} a_0 = \theta_1, \\ a_1 + a_0 = \theta_2, \\ b_0 = \phi_1, \\ b_1 + b_0 = \phi_2, \end{cases}$$

The solution to the linear system is

$$\begin{cases} a_0 = \theta_1, \\ a_1 = \theta_2 - \theta_1, \\ b_0 = \phi_1, \\ b_1 = \phi_2 - \phi_1. \end{cases}$$

When a_0, a_1, b_0 and b_1 have been obtained, the interpolating unit tangent vector field is computed by Eq. (2.1).

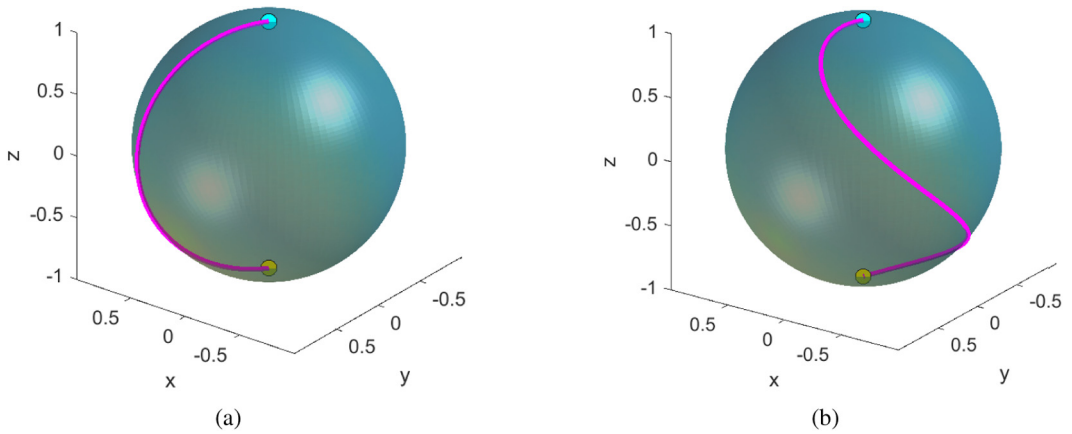

Fig. 2. A sphere curve that interpolates two given unit vectors lying at north pole or south pole of the Gaussian sphere. (a) Azimuthal angles $\phi_1 = 0.3\pi$ and $\phi_2 = 0.3\pi$; (b) azimuthal angles $\phi_1 = 0.3\pi$ and $\phi_2 = 1.4\pi$.

From the above process we know that there exists an interpolating sphere curve for any two distinct points $\mathbf{T}_1$ and $\mathbf{T}_2$ on the unit sphere. Particularly, the interpolating curve is part of a latitude when $\theta_1 = \theta_2$, or the curve is part of a longitude when $\phi_1 = \phi_2$. If $\mathbf{T}_1$ and $\mathbf{T}_2$ are located at the north pole and south pole, respectively, the interpolating curve is a longitude when the angles ϕ_1 and ϕ_2 are chosen the same value. Fig. 2 illustrates two spherical curves that interpolate two sphere poles with different choices of angles ϕ_1 and ϕ_2.

As discussed in Section 2, the unit tangent vector field $\mathbf{T}(\xi)$ lies on a plane that passes through the origin only when $\theta_1 = \theta_2 = 0$ or $\phi_1 = \phi_2$. If this is the case, a planar interpolating ATPH curve can be computed by the method presented in [23]. In the following subsection we construct G^1 interpolating ATPH curves under the assumption that the boundary parameters satisfy $\theta_1^2 + \theta_2^2 \neq 0$ and $\phi_1 \neq \phi_2$ such that $\mathbf{T}(\xi)$ is not a planar tangent vector field.

3.2. Compute the G^1 interpolating spatial ATPH curve

When the non-planar unit tangent vector field $\mathbf{T}(\xi)$ has been obtained, the G^1 interpolating spatial ATPH curve can be determined by solving equations $\mathbf{r}(0) = \mathbf{P}_1$ and $\mathbf{r}(1) = \mathbf{P}_2$. Because $\mathbf{r}(0) = \mathbf{r}_0 = \mathbf{P}_1$, the unknown coefficients of $\rho(\xi)$ within Eq. (2.2) are to be solved based on the following linear system

$$\begin{pmatrix} B_x & -2B_x + 2C_x & B_x - 2C_x + D_x \\ B_y & -2B_y + 2C_y & B_y - 2C_y + D_y \\ B_z & -2B_z + 2C_z & B_z - 2C_z + D_z \end{pmatrix} \begin{pmatrix} \rho_2 \\ \rho_1 \\ \rho_0 \end{pmatrix} = \begin{pmatrix} 2(x_2 - x_1) \\ 2(y_2 - y_1) \\ z_2 - z_1 \end{pmatrix}, \tag{3.1}$$

where B_x, C_x, D_x, B_y, C_y, D_y, B_z, C_z, and D_z are computed by Eq. (2.5) with $\xi = 1$.

Denote M_a the coefficient matrix of the linear system (3.1). Let

$$m = det \begin{pmatrix} B_x & C_x & D_x \\ B_y & C_y & D_y \\ B_z & C_z & D_z \end{pmatrix}.$$

It yields that $det(M_a) = 2m$. If $m \neq 0$, we have the solution to the linear system (3.1) as follows:

$$\begin{pmatrix} \rho_2 \\ \rho_1 \\ \rho_0 \end{pmatrix} = \begin{pmatrix} B_x & -2B_x + 2C_x & B_x - 2C_x + D_x \\ B_y & -2B_y + 2C_y & B_y - 2C_y + D_y \\ B_z & -2B_z + 2C_z & B_z - 2C_z + D_z \end{pmatrix}^{-1} \begin{pmatrix} 2(x_2 - x_1) \\ 2(y_2 - y_1) \\ z_2 - z_1 \end{pmatrix}. \tag{3.2}$$

In practice, the coefficient matrix of linear system (3.1) always satisfies $det(M_a) \neq 0$ and the unique solution to the system can be computed by (3.2). This can be roughly explained as follows: From Eqs. (2.4) and (2.5) we have

$$\begin{pmatrix} \frac{1}{2}B_x(\xi) \\ \frac{1}{2}B_y(\xi) \\ B_z(\xi) \end{pmatrix} = \int_0^\xi t^2 \mathbf{T}(t)dt, \quad \begin{pmatrix} \frac{1}{2}C_x(\xi) \\ \frac{1}{2}C_y(\xi) \\ C_z(\xi) \end{pmatrix} = \int_0^\xi t\mathbf{T}(t)dt, \quad \begin{pmatrix} \frac{1}{2}D_x(\xi) \\ \frac{1}{2}D_y(\xi) \\ D_z(\xi) \end{pmatrix} = \int_0^\xi \mathbf{T}(t)dt.$$

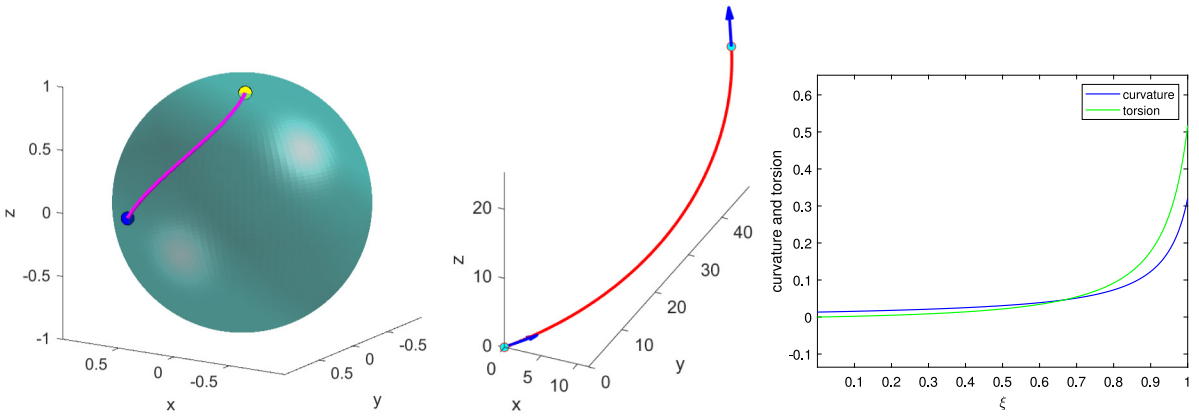

(a) (b) (c)

Fig. 3. G^1 Hermite interpolation: $\mathbf{P}_1 = (0, 0, 0)$, $\mathbf{P}_2 = (9.75, 47, 20.5)$, $\theta_1 = 0$, $\theta_2 = 0.4\pi$, $\phi_1 = \pi/3$, $\phi_2 = 0.7\pi$. (a) The sphere curve that interpolates the given unit tangent vectors on the Gaussian sphere; (b) the G^1 Hermite interpolating curve; (c) the curvature and the torsion plots of the interpolating curve.

It is clear that the functions on the right side of the above three equations are linear independent. Let

$$m_{II}(\xi) = det \begin{pmatrix} \frac{1}{2}B_x(\xi) & \frac{1}{2}C_x(\xi) & \frac{1}{2}D_x(\xi) \\ \frac{1}{2}B_y(\xi) & \frac{1}{2}C_y(\xi) & \frac{1}{2}D_y(\xi) \\ B_z(\xi) & C_z(\xi) & D_z(\xi) \end{pmatrix}.$$

Then, the function $m_{II}(\xi)$ does not identically equal to zero for any parameter interval. Finding the zeros of $m_{II}(\xi)$ is complex and is beyond the algorithm proposed in this paper. In all examples we have experimented we have $m_{II}(1) = \frac{1}{4}m \neq 0$ and the interpolating curves can be obtained by the proposed algorithm. In case $m_{II}(1)$ vanishes, one can still construct an interpolating curve from the equation $\mathbf{r}(\xi_1) = \mathbf{P}_2$ with $\xi_1 \neq 1$.

To check whether or not the interpolating ATPH curve is regular, we should only check the sign of the quadratic function $\rho_{II}(\xi) = \rho_0 B_0^2(\xi) + \rho_1 B_1^2(\xi) + \rho_2 B_2^2(\xi)$, $\xi \in [0, 1]$. Because $\min\{\rho_0, \rho_1, \rho_2\} \leq \rho_{II}(\xi) \leq \max\{\rho_0, \rho_1, \rho_2\}$ for $0 \leq \xi \leq 1$, we have $\rho_{II}(\xi) > 0$ for $\xi \in [0, 1]$, when all ρ_0, ρ_1 and ρ_2 are positive numbers, or, $\rho_{II}(\xi) < 0$ over the domain $[0, 1]$, when all of ρ_0, ρ_1 and ρ_2 are negative. Based on Proposition 1, the obtained interpolating spatial PH curve is regular when the signs of ρ_0, ρ_1 and ρ_2 are the same. It should be noted that the obtained ATPH curves have opposite tangent direction with $\mathbf{T}(\xi)$ when all coefficients ρ_0, ρ_1 and ρ_2 are negative.

Fig. 3 illustrates an example of G^1 Hermite interpolation by the proposed algorithm. A sphere curve is first obtained by interpolating two prescribed points on the unit sphere (see Fig. 3(a)). Then, based on the position condition, a regular interpolating spatial ATPH curve is obtained by solving a simple linear system; see Fig. 3(b) for the obtained interpolating curve. Fig. 3(c) shows the curvature and torsion of the interpolating curve.

Given the Hermite data, $\mathbf{P}_1 \neq \mathbf{P}_2$, and $\mathbf{T}_1 = \mathbf{T}_2$, if $\mathbf{T}_1$ and $\mathbf{T}_2$ are parallel to the vector $\mathbf{P}_2 - \mathbf{P}_1$, it is obvious that the unit tangent vector field $\mathbf{T}(\xi) \equiv \mathbf{T}_1$. Therefore, the interpolating curve is just a straight line. Otherwise, if $\mathbf{T}_1 = \mathbf{T}_2$ is not parallel to the vector $\mathbf{P}_2 - \mathbf{P}_1$, we assume that $\phi_2 - \phi_1 = 2\pi$ and $\theta_1 = \theta_2 \neq 0$. Thus, the interpolating sphere curve is just a latitude other than the equator (see Fig. 4(a)). Fig. 4(b) illustrates the final interpolating ATPH curve.

4. G^1 Hermite Interpolation by ATPH curves with prescribed arc lengths

In this section, we consider the problem of G^1 Hermite interpolation subject to arc length constraint. Besides the G^1 Hermite data $\{\mathbf{P}_1, \mathbf{T}_1; \mathbf{P}_2, \mathbf{T}_2\}$, the arc length L of an interpolating curve has also been given. Using the same technique of tangent vector interpolation described in Section 3, we first construct a sphere curve $\mathbf{T}(\xi)$ that interpolates vectors $\mathbf{T}_1$ and $\mathbf{T}_2$ at the ends. After then, we choose $\rho_{III}(\xi) = l_0 B_0^3(\xi) + l_1 B_1^3(\xi) + l_2 B_2^3(\xi) + l_3 B_3^3(\xi)$ for the construction of G^1 interpolating ATPH curve with arc length constraint.

After the interpolation of unit tangent vector field, the G^1 Hermite interpolation subject to arc length constraint can be formulated as $\mathbf{r}(0) = \mathbf{r}_0 = \mathbf{P}_1$, $\mathbf{r}(1) = \mathbf{P}_2$ and $\int_0^1 \rho(t)dt = L$. The equations can be further reformulated as follows:

$$\begin{pmatrix} G_{11} & G_{12} & G_{13} & G_{14} \\ G_{21} & G_{22} & G_{23} & G_{24} \\ G_{31} & G_{32} & G_{33} & G_{34} \\ 1 & 1 & 1 & 1 \end{pmatrix} \begin{pmatrix} l_3 \\ l_2 \\ l_1 \\ l_0 \end{pmatrix} = \begin{pmatrix} 2(x_2 - x_1) \\ 2(y_2 - y_1) \\ z_2 - z_1 \\ 4L \end{pmatrix}, \tag{4.1}$$

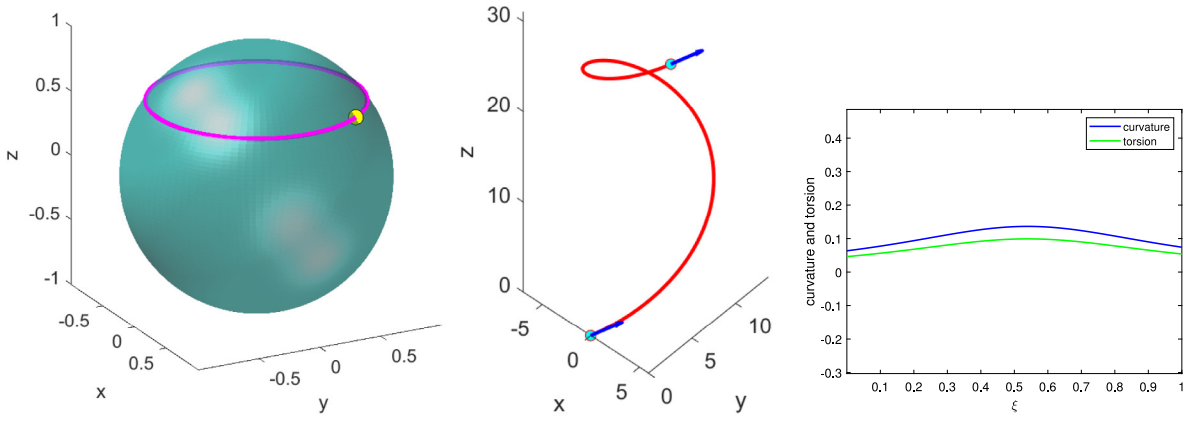

Fig. 4. G^1 Hermite interpolation: $\mathbf{P}_1 = (0, 0, 0)$, $\mathbf{P}_2 = (4, 4.75, 29.25)$, $\theta_1 = 0.2\pi$, $\theta_2 = 0.2\pi$, $\phi_1 = 0.2\pi$, $\phi_2 = 2.2\pi$. (a) The sphere curve that interpolates the given unit tangent vectors on the Gaussian sphere; (b) the G^1 Hermite interpolating curve; (c) the curvature and torsion plot of the interpolating curve.

where G_{11}, G_{12}, G_{13}, G_{14}, G_{21}, G_{22}, G_{23}, G_{24}, G_{31}, G_{32}, G_{33}, and G_{34} are computed by Eqs. (2.5), (2.6) and (2.10) with $\xi = 1$.

Denote M_L the coefficient matrix of the linear system (4.1). Let $q = det(M_L)$. If $q \neq 0$, the solution to the linear system (4.1) is given by

$$\begin{pmatrix} l_3 \\ l_2 \\ l_1 \\ l_0 \end{pmatrix} = \begin{pmatrix} G_{11} & G_{12} & G_{13} & G_{14} \\ G_{21} & G_{22} & G_{23} & G_{24} \\ G_{31} & G_{32} & G_{33} & G_{34} \\ 1 & 1 & 1 & 1 \end{pmatrix}^{-1} \begin{pmatrix} 2(x_2 - x_1) \\ 2(y_2 - y_1) \\ z_2 - z_1 \\ 4L \end{pmatrix}. \tag{4.2}$$

We now explain roughly that Eq. (4.2) does work well for practical curve interpolation. Let $\bar{\mathbf{T}}(t) = (\mathbf{T}_x(t), \mathbf{T}_y(t), \mathbf{T}_z(t), 1)^T$. The Cartesian coordinates and arc length of an integral defined curve with tangent vector field $\mathbf{T}(t)$ are given by

$$\begin{aligned} \bar{\mathbf{r}}(\xi) &= \begin{pmatrix} x(\xi) \\ y(\xi) \\ z(\xi) \\ L(\xi) \end{pmatrix} \\ &= \int_0^\xi \rho_{III}(t)\bar{\mathbf{T}}(t)dt \\ &= l_3 \int_0^\xi B_3^3(t)\bar{\mathbf{T}}(t)dt + l_2 \int_0^\xi B_2^3(t)\bar{\mathbf{T}}(t)dt + l_1 \int_0^\xi B_1^3(t)\bar{\mathbf{T}}(t)dt + l_0 \int_0^\xi B_0^3(t)\bar{\mathbf{T}}(t)dt. \end{aligned} \tag{4.3}$$

Since functions $B_i^3(t)$, $i = 0, 1, 2, 3$, are linear independent, the vector functions $\int_0^\xi B_i^3(t)\bar{\mathbf{T}}(t)dt$, $i = 0, 1, 2, 3$, are also linear independent. On the other hand, using the notations of Eqs. (2.10), (4.3) can be reformulated as

$$\bar{\mathbf{r}}(\xi) = \begin{pmatrix} \frac{1}{2}G_{11}(\xi) & \frac{1}{2}G_{12}(\xi) & \frac{1}{2}G_{13}(\xi) & \frac{1}{2}G_{14}(\xi) \\ \frac{1}{2}G_{21}(\xi) & \frac{1}{2}G_{22}(\xi) & \frac{1}{2}G_{23}(\xi) & \frac{1}{2}G_{24}(\xi) \\ G_{31}(\xi) & G_{32}(\xi) & G_{33}(\xi) & G_{34}(\xi) \\ J_3(\xi) & J_2(\xi) & J_1(\xi) & J_0(\xi) \end{pmatrix} \begin{pmatrix} l_3 \\ l_2 \\ l_1 \\ l_0 \end{pmatrix},$$

where $J_i(\xi) = \int_0^\xi B_i^3(t)dt$, $i = 0, 1, 2, 3$.

Let

$$m_{III}(\xi) = det \begin{pmatrix} \frac{1}{2}G_{11}(\xi) & \frac{1}{2}G_{12}(\xi) & \frac{1}{2}G_{13}(\xi) & \frac{1}{2}G_{14}(\xi) \\ \frac{1}{2}G_{21}(\xi) & \frac{1}{2}G_{22}(\xi) & \frac{1}{2}G_{23}(\xi) & \frac{1}{2}G_{24}(\xi) \\ G_{31}(\xi) & G_{32}(\xi) & G_{33}(\xi) & G_{34}(\xi) \\ J_3(\xi) & J_2(\xi) & J_1(\xi) & J_0(\xi) \end{pmatrix}.$$

Since the four column vectors within the above matrix are linear independent, the function $m_{III}(\xi)$ is not identically equal to zero when ξ belongs to any parameter interval. With simple computation we know that $m_{III}(1) = \frac{1}{16}det(M_L)$. Therefore,

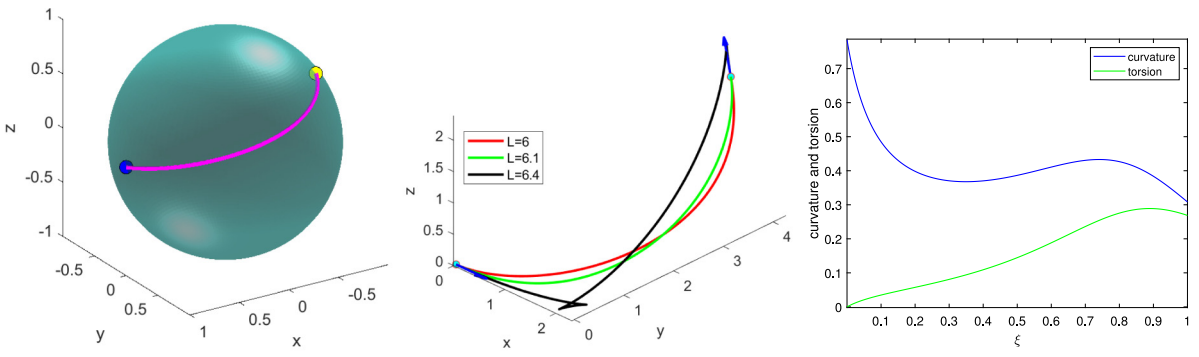

Fig. 5. G^1 Hermite interpolation with prescribed arc lengths. The boundary data are $\mathbf{P}_1 = (0,0,0)$, $\mathbf{P}_2 = (1.5,4,2)$, $\mathbf{T}_1 = (1,0,0)$, and $\mathbf{T}_2 = (-3,2,3)/\sqrt{22}$. (a) The sphere curve that interpolates the given boundary tangents on the Gaussian sphere; (b) the interpolating curves with various prescribed arc lengths; (c) the curvature and torsion plots of the interpolating curve with arc length $L = 6$.

if $m_{III}(1)$ does not vanish, the linear system (4.1) has a unique solution. Due to its complexity, the zeros of $m_{III}(\xi)$ can only be obtained by numerical method at present. Instead of estimating the zeros of $m_{III}(\xi)$ in advance, we compute $m_{III}(1)$ or $det(M_L)$ directly. In our experiments, $m_{III}(1)$ does not vanish and the interpolation curves with prescribed arc lengths can always be obtained by solving linear system (4.1). In case $m_{III}(1) = 0$, one can compute the interpolating curve by choosing a different parameter for interpolation of the boundary data.

An interpolating curve with prescribed arc length is obtained by Eqs. (2.10) and (4.2) when the linear system (4.1) has a solution. However, based on Proposition 1 we know that the interpolating curve is regular over the domain only when the cubic function $\rho(\xi)$ satisfies $\rho(\xi) \neq 0$ for all $\xi \in [0,1]$. We present here a sufficient condition for checking the regularity of the obtained interpolating ATPH curve. Recall that the scaling function is $\rho_{III}(\xi) = l_0 B_0^3(\xi) + l_1 B_1^3(\xi) + l_2 B_2^3(\xi) + l_3 B_3^3(\xi)$, $\xi \in [0,1]$. If l_0, l_1, l_2 and l_3 are all positive numbers, the inequality $\rho(\xi) > 0$ holds over the domain. Similarly, if l_0, l_1, l_2 and l_3 are negative numbers, $\rho(\xi) < 0$ for $\xi \in [0,1]$. Consequently, when one of the above conditions is satisfied, it is guaranteed that the integral curve is regular.

Fig. 5 illustrates an example of G^1 Hermite interpolation with arc length constraint. For the given boundary data, a sphere curve that interpolates given boundary tangents on the Gaussian sphere is first computed. Then, interpolating ATPH curves are obtained by solving linear system (4.1) under the constraint of prescribed arc lengths. From Fig. 5(b) we know that the interpolating curves are regular when the sign of the function $\rho_{III}(\xi)$ does not change for $\xi \in [0,1]$. It is also known that the function $\rho_{III}(\xi)$ can have zeros within the interval [0,1] and the interpolating ATPH curve can have singular points when the arc length has not been properly chosen. Fig. 5(c) illustrates the curvature plot and torsion plot of the interpolating ATPH curve with arc length $L = 6$.

5. Examples

In this section, we present several examples for the construction of G^1 Hermite interpolating ATPH curves. Given a sequence of points $\mathbf{P}_i \in \mathbb{R}^3$, $i = 0,\ldots,n$, and unit tangents $\mathbf{T}_i$, $i = 0,\ldots,n$, at the points, we construct a G^1 interpolating ATPH curve to each pair of consecutive points and tangents. As a result, an interpolating spatial ATPH spline curve with G^1 continuity is obtained.

First, we sample points and unit tangents on a cylinder curve $\mathbf{r}(t) = (4\cos t, 4\sin t, 0.2t^2)$, $t \in [0, 2\pi]$. The Hermite data are sampled from the curve at $t_i = \frac{2i\pi}{n}$, $i = 0,\ldots,n$. Particularly, we chose $n = 2, 4, 8, 16$ for the construction of interpolating ATPH spline curves by the algorithm given in Section 3. Fig. 6 illustrates two examples of ATPH spline curve interpolation when $n = 2$ or $n = 4$. The maximum approximation errors and the maximum angle differences of tangent vectors between the interpolating curves and the original curve are given in Table 1. From the table we can see that more accurate approximating results can be obtained when many more sampled points and tangents are interpolated by regular ATPH curves. As a comparison, we have also interpolated the same set of sampled points and tangents by G^1 cubic polynomial PH spline curves [24]. It can be observed that the ATPH curves can approximate the original curve with even higher accuracy than the cubic PH curves. The curvature plots and the torsion plots of the interpolating curves also show the higher quality of the proposed ATPH curves.

Second, we construct ATPH spline curves by interpolating points and tangents sampled from a segment of helix on the elliptic cylinder $\mathbf{r}(t) = (2\cos t, 2.5\sin t, t)$, $t \in [0, 2\pi]$. Assume that points and unit tangent vectors have been sampled from the curve at $t_i = \frac{2i\pi}{4}$, $i = 0, 1, 2, 3, 4$. Fig. 7 illustrates the interpolating spline curves consisting of 4 pieces of spatial ATPH curves or 4 pieces of cubic PH curves. Though both of the two types of interpolating curves approximate the original curve very well, it is observed that the interpolating ATPH curves are fairer than the cubic PH curves because the former have even fewer number of curvature extremes or torsion extremes.

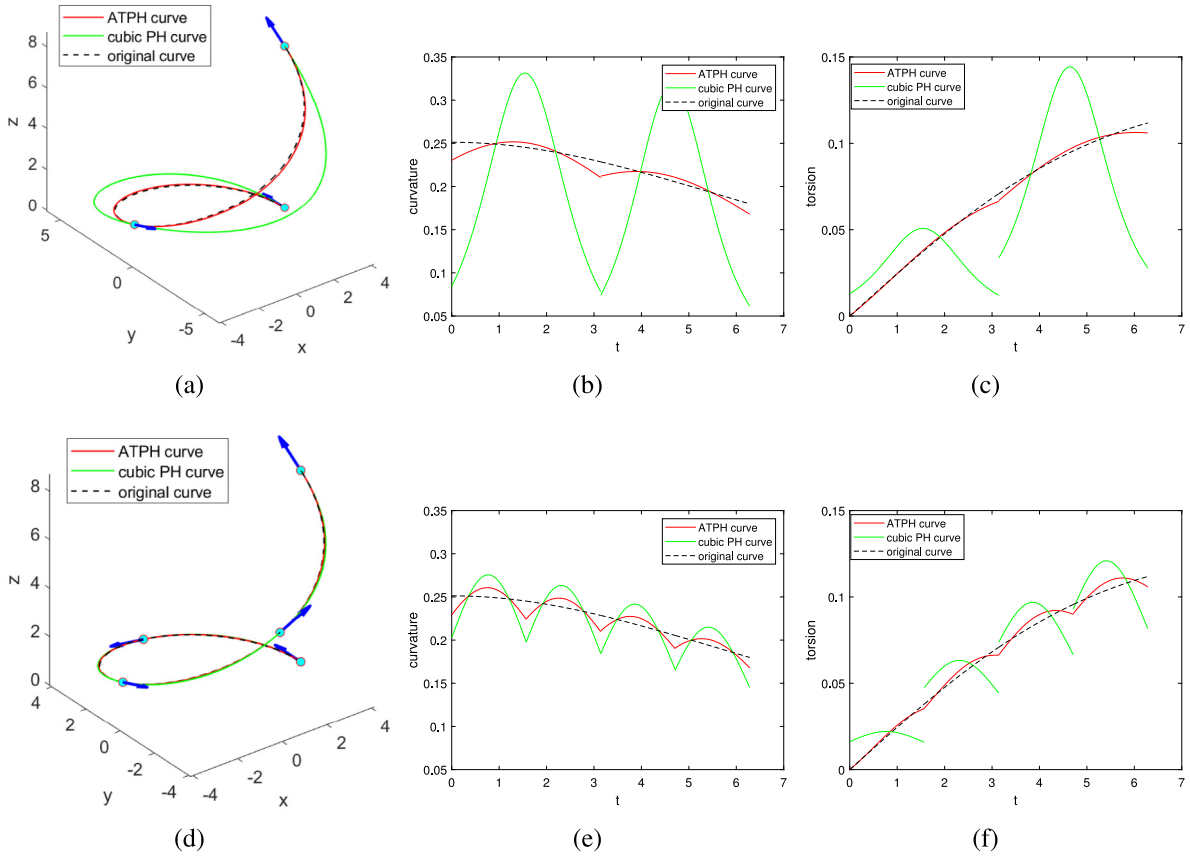

Fig. 6. Interpolation of points and tangents sampled from a spatial curve on a cylinder by splines of ATPH curves or splines of cubic PH curves. (a) The 2 pieces of interpolating curves; (b) the corresponding plot of the curvature of (a); (c) the corresponding plot of the torsion of (a); (d) the 4 pieces of interpolating curves; (e) the corresponding plot of the curvature of (d); (f) the corresponding plot of the torsion of (d). ATPH curves, cubic PH curves and original curves are drawn in red, green, and black, respectively. (For interpretation of the references to color in this figure legend, the reader is referred to the web version of this article.)

Table 1
The maximum approximation errors and the maximum angle differences of tangent vectors for different sets of interpolating ATPH curves.

#segments	Max approx. error	Max tangent angle difference
2	0.137872	0.007688
4	0.061317	0.001995
8	0.029884	5.003854E−4
16	0.014849	1.251672E−4

6. Conclusions and discussions

In this paper we have defined a family of spatial ATPH curves based on the integral of scaled unit tangent vector fields. Using sphere curves represented by sphere coordinates and polynomial scaling functions, the Cartesian coordinates of the ATPH curves can be computed explicitly. These types of ATPH curves have polynomial arc lengths and can be used to represent several types of typical curves in non-rational form. For given G^1 Hermite boundary data together with or without a prescribed arc length, the interpolating ATPH curves can be obtained by solving simple linear systems. Unlike Hermite interpolation by conventional PH curves, the proposed geometric Hermite interpolation has unique solutions and the regularity of the interpolating curves can be checked easily just based on the signs of the obtained scaling factors within the hodographs. For practical applications, if an obtained interpolating ATPH curve is not regular, one can adjust the input data to compute a new interpolation curve or use other types of curves such as space biarcs to interpolate the geometric Hermite data.

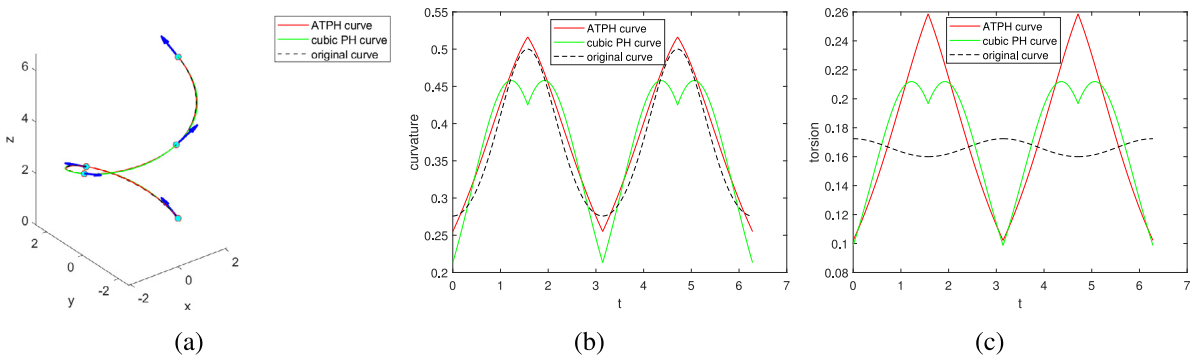

Fig. 7. (a) G^1 ATPH spline curve or G^1 cubic PH spline curve that interpolate points and tangents sampled from a helix on an elliptic cylinder; (b) the curvature plots of the interpolating curves; (c) the torsion plots of the interpolating curves.

Acknowledgments

We owe thanks to the anonymous referees whose comments and suggestions helped to improve the clarity of the paper greatly. This work is supported by the National Natural Science Foundation of China grants (11290142).

References

[1] R.T. Farouki, T. Sakkalis, Pythagorean hodographs, IBM J. Res. Dev. 34 (5) (1990) 736–752.
[2] M. Byrtus, B. Bastl, G^1 Hermite Interpolation by PH cubics revisited, Comput. Aided Geom. Design 27 (8) (2010) 622–630.
[3] B. Bastl, K. Slabá, M. Byrtus, Planar C^1 Hermite interpolation with uniform and non-uniform TC-biarcs, J. Comput. Appl. Math. 30 (1) (2013) 58–77.
[4] R.T. Farouki, C.A. Neff, Hermite interpolantion by Pythagrean hodograph quintics, Math. Comp. 64 (212) (1995) 1589–1609.
[5] R.T. Farouki, Z. Sír, Rational Pythagorean-hodograph space curves, Comput. Aided Geom. Design 28 (2) (2011) 75–88.
[6] W. Lü, Offset-rational parametric plane curves, Comput. Aided Geom. Design 12 (6) (1995) 601–616.
[7] H. Pottmann, Curve design with rational Pythagorean-hodograph curves, Adv. Comput. Math. 3 (1–2) (1995) 147–170.
[8] X. Yang, Geometric interpolation by PH curves with quadratic or quartic rational normals, Comput. Aided Des. 114 (2019) 112–121.
[9] R.T. Farouki, Pythagorean-Hodograph Curves: Algebra and Geometry Inseparable, Springer, Berlin, 2008, p. 26.
[10] J. Kosinka, M. Lávicka, Pythagorean hodograph curves: A survey of recent advances, J. Geom. Graph. 18 (1) (2014) 23–43.
[11] L. Piegl, W. Tiller, The NURBS Book, Springer-Verlag New York, 1997.
[12] H. Pottmann, The geometry of Tchebycheffian splines, Comput. Aided Geom. Design 10 (3–4) (1993) 181–210.
[13] H. Pottmann, M.G. Wagner, Helix splines as an example of affine Tchebycheffian splines., Adv. Comput. Math. 2 (1) (1994) 123–142.
[14] J. Zhang, C-curves: An extension of cubic curves, Comput. Aided Geom. Design 13 (3) (1996) 199–217.
[15] J. Zhang, Two different forms of C-B-splines, Comput. Aided Geom. Design 14 (1) (1997) 31–41.
[16] Q. Chen, G. Wang, A class of Bézier-like curves, Comput. Aided Geom. Design 20 (1) (2003) 29–39.
[17] E. Mainar, J.M. Peña, Optimal bases for a class of mixed spaces and their associated spline spaces, Comput. Math. Appl. 59 (4) (2010) 1509–1523.
[18] G. Wang, M. Fang, Unified and extended form of three types of splines, J. Comput. Appl. Math. 216 (2) (2008) 498–508.
[19] W. Shen, G. Wang, Geometric shapes of C-Bézier curves, Comput. Aided Des. 58 (2015) 242–247.
[20] L. Romani, L. Saini, G. Albrecht, Algebraic-Trigonometric Pythagorean-Hodograph curves and their use for Hermite interpolation, Adv. Comput. Math. 40 (5–6) (2014) 977–1010.
[21] C. González, G. Albrecht, M. Paluszny, M. Lentini, Design of C^2 algebraic-trigonometric Pythagorean hodograph splines with shape parameters, Comput. Appl. Math. 37 (2) (2018) 1472–1495.
[22] L. Romani, F. Montagner, Algebraic-Trigonometric Pythagorean-Hodograph space curves, Adv. Comput. Math. 45 (2019) 75–98.
[23] W. Wu, X. Yang, Geometric Hermite interpolation by a family of intrinsically defined planar curves, Comput. Aided Des. 77 (2016) 86–97.
[24] S.-H. Kwon, Solvability of G^1 Hermite interpolation by spatial Pythagorean-hodograph cubics and its selection scheme, Comput. Aided Geom. Design 27 (2) (2010) 138–149.